inorganics

MDPI

Article

Tetrahydroxidohexaoxidopentaborate(1-) Salts of C_6-Linked Substituted Diimidazolium and Dipyrrolidinium Cations: Synthesis, Characterization and XRD Studies

Ahmad R. Al-Dulayymi [1], Michael A. Beckett [2,*], Radek Braganca [1], Simon J. Coles [3], Peter N. Horton [3] and Thomas A. Rixon [2]

[1] Bio-Composites Centre, Bangor University, Bangor LL57 2UW, UK
[2] School of Environmental and Natural Sciences, Bangor University, Bangor LL57 2UW, UK
[3] School of Chemistry, University of Southampton, Southampton SO17 1BJ, UK
* Correspondence: m.a.beckett@bangor.ac.uk

Abstract: Several tetrahydroxidohexaoxidopentaborate(1-) salts of *N*-substituted diimidazolium cations or *N*-substituted dipyrrolidinium cations linked through *N*-C_6-*N* chains have been synthesized and characterized spectroscopically (NMR, IR) and by single-crystal XRD studies: $[R(NC_3H_3N)(CH_2)_6(NC_3H_3N)R][B_5O_6(OH)_4]_2{\cdot}xH_2O$ (R = Me, x = 0 (**1**); R = Et, x = 3 (**2**); $[Me(NC_3H_3N)(CH_2(C_6H_4)CH_2)(NC_3H_3N)Me][B_5O_6(OH)_4]_2$ (**3**), $[(C_4H_8N)(R)(CH_2)_6(R)(NC_4H_8)][B_5O_6(OH)_4]_2{\cdot}xB(OH)_3$ (R = Me, x = 0 (**4**, two polymorphs); R = Et, x = 0 (**5**); R = Bu, x = 4 (**6**); R = allyl, x = 0 (**7**)). Representative samples (**1** and **7**) were also characterized by thermal (TGA/DSC) studies; compounds are thermally decomposed to B_2O_3 in air. Numerous anion-anion H-bonding interactions are present in the solid-state structures of **1**–**5** and **7** as giant anionic networks. Unusually, in **6** there are no $R_2^2(8)$ anion-anion interactions as the co-crystallized $B(OH)_3$ bridges between all pentaborate anions. H-bonding interactions in **1**–**7** have been examined using Etter graph set analysis; C(8), $C_3^3(18)$, $R_2^2(8)$, $R_2^2(12)$ and $R_4^4(12)$ motifs have been identified.

Keywords: H-bonding; imidazolium; pyrrolidium; pentaborate; tetrahydroxidohexaoxidopeentaborate (1-); XRD

Citation: Al-Dulayymi, A.R.; Beckett, M.A.; Braganca, R.; Coles, S.J.; Horton, P.N.; Rixon, T.A. Tetrahydroxidohexaoxidopentaborate (1-) Salts of C_6-Linked Substituted Diimidazolium and Dipyrrolidinium Cations: Synthesis, Characterization and XRD Studies. *Inorganics* **2024**, *12*, 220. https://doi.org/10.3390/inorganics12080220

Academic Editor: Richard Dronskowski

Received: 22 July 2024
Revised: 9 August 2024
Accepted: 13 August 2024
Published: 15 August 2024

1. Introduction

Boron has a great affinity for oxygen and most naturally occurring boron-containing materials, traditionally referred to as borates, feature boron atoms bound exclusively to oxygen atoms [1–3]. Borates are ionic salts and are a class of compounds that are structurally diverse, with the borate entities comprised of either insular hydrated anions (hydroxidooxidopolyborates) or as more condensed anionic layers (2-D) or nets (3-D) [4–10]. These more condensed units may be hydrated or anhydrous (oxidopolyborates). Some boron-containing materials, e.g., tincalconite ($Na_2B_4O_5(OH)_4{\cdot}3H_2O$) and synthetic borax pentahydrate ($Na_2B_4O_5(OH)_4{\cdot}3H_2O$), obtained from kernite ($Na_2B_4O_6(OH)_2{\cdot}3H_2O$) or tincal/borax decahydrate ($Na_2B_4O_5(OH)_4{\cdot}8H_2O$), are industrially very important with bulk scale applications in glasses and in ceramic industries [11,12]. There are also many synthetic polyborate analogues and some of these materials, e.g., zinc borate, have large-scale industrial applications [13]. Other synthetic materials have more specialized uses, e.g., β-BBO (β-barium borate) in NLO materials [14]. We have previously studied synthesis and structural aspects of various hydrated oxidoborates with organic [15] phosphonium [15,16] and transition-metal [15,17] cations in order to gain a deeper understanding of the self-assembly processes [18–21] that are involved in their synthesis/crystallization from aqueous solution from the usual starting material, $B(OH)_3$. Several important factors have been identified and these include relative ion sizes [22,23], packing effects [24] and intermolecular/interionic interactions (e.g., H-bonding) [23,24]. The H-bonded anion-anion 3-D lattices found in insular

tetrahydroxoidohexaoxidopentaborate(1-) (hereafter pentaborate in this manuscript [25]) salts are particularly adaptable and in the absence of other driving forces often arise in self-assembled polyborate materials [23]. Recently, our attention has turned to the synthesis of polyborate salts derived from 'choline-like' dications involving C_2/C_3-linked *N*-substituted diaminoalkanes as potential bio-stimulants for agricultural use [26–28]. In these synthetic studies, new tetraborate(2-) and pentaborate salts were prepared and characterized. This general synthetic principle is extended in this manuscript to include C_6-linked dications with either two *N*-substituted imidazolium moieties or two *N*-substituted pyrrolidinium moieties for a similar agricultural bio-stimulant application. This class of compounds may potentially also find applications as wide band-gap semiconductors, fluorescent materials and NLO materials [15,17]. As background, it should be noted that we have previously reported pentaborate salts of substituted pyrrolidinium cations [23,29,30] and of substituted imidazolium cations [29,31]; other workers have also reported pentaborate salts of imidazolium cations [32–34]. Notably, Schubert and co-workers have reported several pentaborate salts and an octaborate(2-) salt from related unsubstituted protonated α,ω-diaminoalkanes (with C_5–C_{12} links) [35] and the triimidazolium nonaborate(3-) salt, $[C_3H_5N_2]_3[B_9O_{12}(OH)_6]$ [36,37]. This manuscript reports on the synthesis and crystallographic characterization of seven new pentaborate salts derived from C_6-linked dications. The structures of the pentaborate anion and the dications present in these new compounds are shown schematically in Figure 1. All compounds were characterized spectroscopically, some by thermal studies, and all by single-crystal XRD analyses. The solid-state H-bonding interactions observed in these new pentaborate salts are described and analysed using Etter terminology [38].

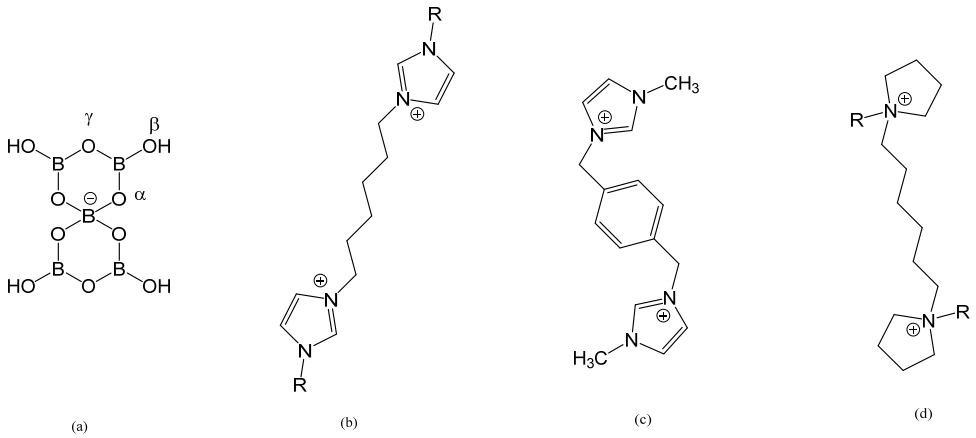

Figure 1. Schematic drawings of the (**a**) tetrahydroxidohexaoxidopentaborate(1-) anion in **1**–**7** and (**b**) the cations in **1** (R = Me) and **2** (R = Et), (**c**) the cation in **3**, and (**d**) the cations in **4** (R = Me), **5** (R = Et), **6** (R = Bu) and **7** (R = Allyl).

2. Results and Discussion

2.1. General and Synthetic Procedures

The new compounds crystallized from aqueous solution in excellent yields. The C_6-linked di(*N*-substituted imidazolium) or di(*N*-substituted pyrrolidinium) dihalides were initially treated with an excess of a suspension of $[OH]^-$ activated ion-exchange resins to afford aqueous solutions containing their dihydroxide salts. After the ion-exchange resins had been removed by filtration, ten equivalents of $B(OH)_3$ were added to each of these solutions. Removal of the solvent after a few hours afforded crude crystalline materials. These crude materials were used for spectroscopic and thermal analysis and could be re-crystallized from aqueous solutions. The formation of dication bis(pentaborate) salts was expected since pentaborate salts have been prepared for related unlinked organic cations following similar synthetic procedures [15,23,31]. As has been noted elsewhere, $B(OH)_3$ provides an easy access to an aqueous dynamic combinatorial library [20,21] of polyborate anions [12,39–41] and pentaborate salts,

templated by the cations present, often crystallized from such solutions as a consequence of the many favourable anion-anion solid-state H-bonding interactions [18,23,24,42]. The H-bonding interactions for **1**–**7** are discussed and analysed in detail in Section 2.3. Compound **6** was a co-crystallized product, $[(C_4H_8N)(Bu)(CH_2)_6(Bu)(NC_4H_8)][B_5O_6(OH)_4]_2{\cdot}4B(OH)_3$, rather than a simple salt. Co-crystallization of $B(OH)_3$ into non-metal cation pentaborate salts is sometimes observed with sterically demanding non-metal cations [22,43–46]. Compound **2** was also a co-crystallized product and is a trihydrate, $[Et(NC_3H_3N)(CH_2)_6(NC_3H_3N)Et][B_5O_6(OH)_4]_2{\cdot}3H_2O$. The role of H_2O in the solid-state lattice of **2** is discussed in Section 2.3. The new compounds were all characterized by spectroscopic (NMR and IR) analysis and by elemental analysis (Section 2.2). Compounds **1** and **7** were also characterized by thermal (TGA/DSC) studies (Section 2.2) as representative examples. All re-crystallized samples gave crystals suitable for X-ray diffraction studies (Section 2.3).

2.2. Spectroscopic and Thermal Analyses

The IR spectra (KBr discs or ATR, ESI: Figures S1–S7) of compounds **1**–**7** showed absorptions due to the organic cations (e.g., unsaturated C-H stretches ca 3100 cm^{-1} (**1**–**3**) and saturated C-H stretches ca. 2980 cm^{-1} (**1**–**7**)). Compounds **1**–**3** showed imidazole ring stretches at ca. 1575 cm^{-1} [47] and all compounds exhibited a series of strong absorptions in the 1400–800 cm^{-1} region mainly associated with B-O stretches and bends of the pentaborate anion [48]. The C-N ring mode stretches associated with the cations would also be expected to occur in this region [47,49]. Of particular relevance is that all samples had a strong B-O stretch between 908–925 cm^{-1}. This band, assigned to the asymmetric B_{tet}-O stretch, is reported as diagnostic for the pentaborate anion [45].

Compounds **1**–**7** were insoluble in the organic solvents $CHCl_3$, CH_2Cl_2, MeOH, EtOH, Et_2O, C_6H_6 and toluene but dissolved, with decomposition of the anion [39], in H_2O. NMR (^1H, ^{13}C and ^{11}B) spectra were recorded for **1**–**7** dissolved in D_2O (ESI: Figures S8–S25). These ^1H and ^{13}C spectra of **1**, **2**, **4**–**7** were consistent with the C_6-linked dications with either *N*-substituted imidazolium moieties (**1**, **2**) or *N*-substituted cationic pyrrolidinium moieties (**4**–**7**) at the end of the 1,6-hexanediyl chains. DEPT spectra were used to help with the assignment of ^{13}C signals. Compound **3** showed ^1H and ^{13}C signals associated with a 1,4-phenylenebis(methylene) group and the cationic imidazolium end groups.

The decomposition of **1**–**7** in aqueous solution is evidenced by their ^{11}B NMR spectra in D_2O. These 'signature' spectra are typical of samples that were originally pentaborate salts with signals at ca. +17, + 13 and +1 with concentration-dependent relative intensities generally close to 85:14:1 [23]. These signals are from three hydroxidooxidoborate species arising from rapidly attained borate/H_2O equilibria [39–41] that occur in aqueous solution: $B(OH)_3/[B(OH)_4]^-$, $[B_3O_3(OH)_4]^-$ and $[B_5O_6(OH)_4]^-$, respectively. The signal at +1 ppm is associated with the 4-coordinate boron centre of $[B_5O_6(OH)_4]^-$ whereas signals at +13 are attributed to the 3-coordinate borons of $[B_3O_3(OH)_4]^-$ [39]. These equilibria are also important in the synthesis of **1**–**7** since they are involved in the formation of the hydroxidooxidopolyborate DCL [21] from $B(OH)_3$ in the reaction solution and from which the templating cation affects crystallization.

Thermal (TGA/DSC) studies for pentaborate(1-) salts are well documented in the literature [15,29,35,50–54]. These generally proceed via (i) a low temperature step (<150 °C) involving endothermic removal of interstitial/co-crystallized H_2O, (ii) at intermediate temperatures (200–250 °C) further endothermic loss of two H_2O per $[B_5O_6(OH)_4]^-$ anion with formation of an anhydrous pentaborate $[B_5O_8]^-$, and (iii) at higher temperatures (400–800 °C), exothermic oxidation of the organic cation with the formation of $2.5B_2O_3$ per $[B_5O_6(OH)_4]^-$ anion.

Thermal analysis of **1**, a pentaborate salt containing two imidazolium(1+) C_6-linked centres was undertaken as representative of **1**–**3**. Compound **1** is thermally decomposed in air over the temperature range 250–400 °C, with loss of $4H_2O$ as a result of condensation of the pentaborate network to afford the anhydrous pentaborate. Further heating to higher temperatures (800 °C) affords a residue with a mass corresponding to $5B_2O_3$ as the organic

cation is oxidized (ESI Figure S26). Likewise, thermal analysis of **7**, a pentaborate salt containing two pyrrolidinium(1+) C_6-linked centres was undertaken as representative of **4**–**7**. The TGA trace did not show a standard two-step process but rather a continuous loss of mass from 100–800 °C; the residual mass was consistent with $5B_2O_3$; condensation with loss of $4H_2O$ and oxidation of the cation were not differentiated in this example (ESI Figure S27). The thermal behaviour of **1** and **7** are consistent with thermal behaviour reported for other organic cation pentaborate salts [15,29,35,50–54].

2.3. Crystallographic Studies

The cations in **1**–**3** contain two *N*-substituted imidazolium centres. Compounds **1**–**3** are ionic solids with one [C_6-linked diimidazolium]$^{2+}$ dication and two $[B_5O_6(OH)_4]^-$ anions in the formula unit. Additionally, **2** has $3H_2O$ co-crystallized within the formula unit. The C_6-linkage for **1** and **2** is 1,6-hexanediyl whereas for **3** it is 1,4-phenylenebis(methylene). Compounds **1** and **3** have *N*-methyl substituents on the imidazole rings whilst **2** has *N*-ethyl substituents. Crystallographically, the cations in **1** and **3** are centrosymmetric and the two pentaborate anions are equivalent. This is not the case for **2** where all atoms of the cation are unique and the two pentaborate anions also differ. Drawings of the structures of **1**–**3** are given in Figure 2 together with details of their crystallographic atomic labels.

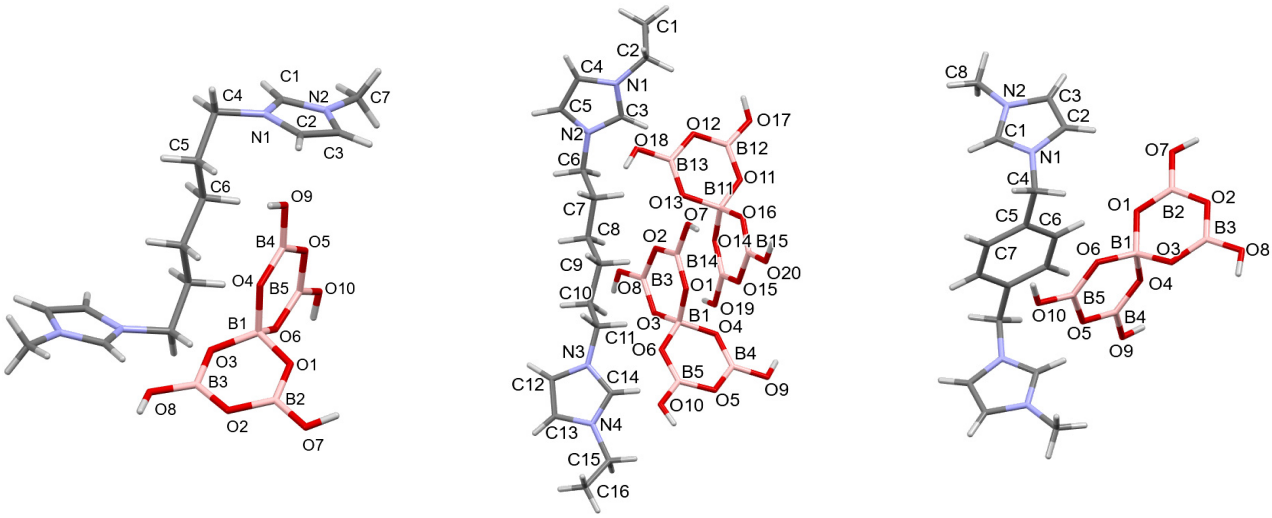

(**a**) (**b**) (**c**)

Figure 2. Drawings of the structures of the imidazolium-based cations and the pentaborate anions present in (**a**) $[Me(NC_3H_3N)(CH_2)_6(NC_3H_3N)Me][B_5O_6(OH)_4]_2$ (**1**), (**b**) $[Et(NC_3H_3N)(CH_2)_6(NC_3H_3N)Et][B_5O_6(OH)_4]_2{\cdot}3H_2O$ (**2**), and (**c**) $[Me(NC_3H_3N)(CH_2(C_6H_4)CH_2)(NC_3H_3N)Me][B_5O_6(OH)_4]_2$ (**3**), showing selected crystallographic atomic labels. The cations in **1** and **3** are centrosymmetric. The three H_2O in **2** are also omitted for clarity. Full crystallographic atomic labelling is available in the ESI.

The bond distances and internuclear bond angles for the imidazolium units in the dications in **1**–**3** are similar to those reported for unlinked imidazolium cations [31–34,36,37]. The conformation of the dications resembles that of weightlifters' dumbbells with a linear 'bar' between two sterically more-demanding cationic heads. The 1,6-hexanediyl bars in **1** and **2** adopt staggered 'zig-zag' conformations. The bond angles and bond distances within the pentaborate anions of **1**–**3** are within the ranges reported for other pentaborate salts and compounds containing boroxole rings with both 3- and 4-coordinate boron centres [15,17]. Thus, the OBO angles from 3-coordinate 'trigonal plane' boron centres [116.71(10)–122.00(10)° (**1**); 115.74(15)–122.70(15)° (**2**); 116.41(7)–122.05(7)° (**3**)] are larger than those involving the 4-coordinate 'tetrahedral' boron centres [107.90(9)–111.23(9)° (**1**); 107.30(12)–111.90(13)° (**2**); 107.46(6)–111.43(6)° (**3**)]. The deviations in the angles for the

'tetrahedral' boron centres from the idealized 109.5° demonstrate that they are distorted tetrahedra and this can be quantified using τ_4 [55] and *THC* [56] values. The calculated τ_4 values are all 0.98 and close to the value of 1.0 expected for undistorted tetrahedral geometries. Likewise, *THC*/100 values for the tetrahedral centres are 0.934 (**1**), 0.930 (**2**, B1) and 0.927 (**2**, B11), and 0.914 (**3**) indicating some distortion from ideal (1.00). B-O distances involving 3-coordinate B centres [1.3573(14)–1.3857(14) Å (**1**); 1.353(2)–1.394(2) Å (**2**); 1.3499(9)–1.3859(9) Å (**3**)] are shorter than those involving the 4-coordinate boron centres [1.4515(14)–1.4783(14) Å (**1**); 1.443(2)–1.486(2) Å (**2**); 1.4559(9)–1.4811(9) Å (**3**)]. The ranges of the boroxole ring BOB angles are 118.67(9)–123.16(9)° (**1**), 118.76(13)–123.92(13)° (**2**) and 118.71(6)-123.67(6)° (**3**) indicating possible sp^2 hybridization for these ring oxygen atoms [57].

H-bonding interactions (particularly anion-anion rather than cation-anion) generally play an important role in stabilizing solid-state structures of pentaborate salts [15,23]. Compound **1** does not form cation-anion H-bond interactions and its interactions are restricted to strong structure-defining anion-anion interactions. In **1** and **3** each pentaborate anion forms 4 donor H-bond interactions to four neighbouring pentaborate anions at, using terminology defined by Schubert and co-workers [35] (see Figure 1a), three α and one β acceptor sites, or ααaβ. Both compounds **1** and **3** have known, but different, 3-D H-bonded anionic lattices with that of **1** previously described as herringbone [15,29]. Using Etter graph set terminology [38], the three α-interactions in both **1** and **3** are $R_2^2(8)$ whilst the β-interactions differ and are part of infinite C(8) chains in **1** and centrosymmetric $R_2^2(12)$ rings in **3**. The $R_2^2(8)$ interactions in **1** originate from O7H7, O9H9 and O10H10 with acceptor sites at O4′, O1′, O6′, respectively, whilst the C(8) interaction involves O8H8···O10′. The $R_2^2(8)$ α-interaction {-O10H10···O6′B5′O10′H10′···O6B5-} is reciprocal, i.e., centrosymmetric. The $R_2^2(8)$ interactions in **3** originate from O8H8, O9H9, O10H10 with acceptor sites at O3′, O4′ and O6′, respectively, whilst the reciprocal $R_2^2(12)$ interaction involves O7H7···O8′ (Figure 3). All three $R_2^2(8)$ interactions in **3** are reciprocal. Interestingly, the imidazolium cations in **3** are involved in H-bond donor interactions to β-OH sites of pentaborate anions: C1H1···O9 (Figure 3). This interaction has a donor (C) acceptor (O) distance of 3.0475(9) Å. The cations in **1** and **3** are situated, running lengthwise, within the large channels of the anionic lattice.

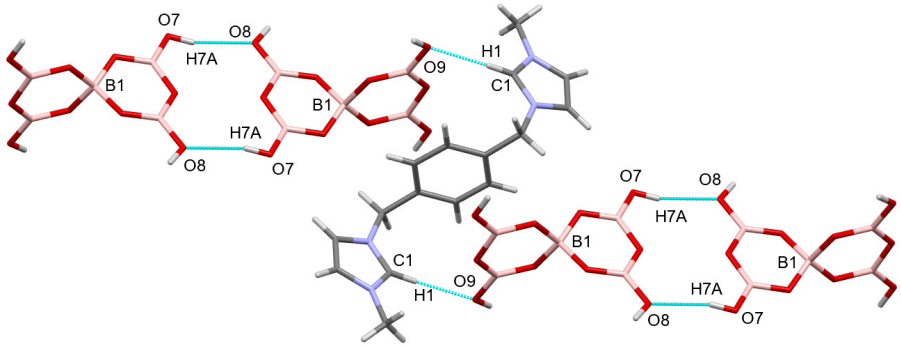

Figure 3. Diagram showing some of the H-bond interactions in $[Me(NC_3H_3N)(CH_2(C_6H_4)CH_2)(NC_3H_3N)Me][B_5O_6(OH)_4]_2$ (**3**): H-bonds originating from the imidazolium rings (C1H1···O9) and the reciprocal $R_2^2(12)$ motif involving pentaborate anions (O7H7A···O8′). The three remaining pentaborate hydroxy groups are involved as donors in reciprocal $R_2^2(8)$ H-bonding.

Compound **2** has three H_2O molecules co-crystallized per dication; two of these H_2O molecules (containing O22 and O23) are disordered over two sites with s.o.fs.of 0.5. The H-bonding donor interactions of the two crystallographically independent pentaborate units are different: the anion containing B1 forms three $R_2^2(8)$ α-interactions and a donor H-bond to an H_2O molecule (O21, s.o.f. 1.0). H_2O acceptor sites in polyborate networks have been described as ω [44] and this B1 containing pentaborate can be considered an ααaω donor. The anion containing B11 forms 3 $R_2^2(8)$ α-interactions and a β-interaction

(ααaβ). The $R_2^2(8)$ interactions that originate from O7H7, O8H8, O9H9, O18H18, O19H19, O20H20 have acceptor sites at O14, O16, O13, O4, O1, and O3, respectively, whilst the β-interaction is O17H17···O7. This β-interaction is part of infinite chains that link the crystallographically independent pentaborate anions and the H_2O molecule (O21), e.g., {-O17H17···O7B2O1B1O6B5O10H10···O21H21···O19B14O14B11O11B12-}$_n$ with the Etter symbol of $C_3^3(18)$ (Figure 4, also see Figure 2b for full atomic labels of **2**). The H_2O containing O21 is also a H-bond donor to the disordered H_2O molecules containing O22/O22A. The two disordered H_2O molecules (containing O22/O22A and O23/O23A) are not H-bond acceptors from the pentaborates but contribute to the H-bonding lattice by donation to β-sites of the pentaborates (O22H22A and O22AH22D to O9 and O23H23 and O23AH23D to O20). Overall, the structure of **2** is very similar to a standard brick wall structure [15,29] but with two C(8) chains replaced with larger $C_3^3(18)$ chains by inclusion of an H_2O molecule into a now-expanded anionic lattice. The cations in **2** have dumbbell conformations (See Figure 2b) and the large channels of the lattice can accommodate two cations. The cations are arranged as offset lengthwise chains with imidazolium π-stacking interactions between them to further stabilize the structure.

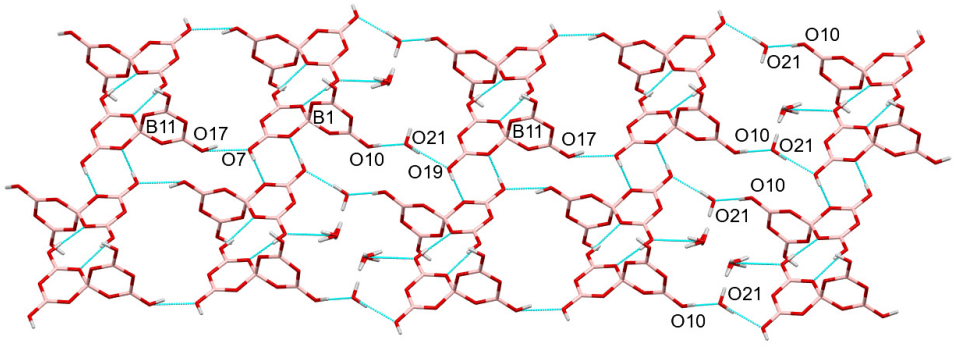

Figure 4. A partial view down the *b* axis of $[Et(NC_3H_3N)(CH_2)_6(NC_3H_3N)Et][B_5O_6(OH)_4]_2{\cdot}3H_2O$ (**2**), showing four horizontal chains of pentaborate anions linked by a water molecule (O21). The chains have alternating pentaborate anions (see positions of the B1 and B11 labels) and adjacent chains alternate in direction (see O10 and O21 labels). The repeating infinite chain has the Etter symbol $C_3^3(18)$.

The cations in **4**–**7** all contain two *N*-substituted pyrrolidinium centres. Compounds **4**–**7** are ionic solids with one [C_6-linked dipyrrolidinium]$^{2+}$ dication and two $[B_5O_6(OH)_4]^-$ anions in the formula unit. Additionally, **6** is a co-crystal with $4B(OH)_3$ within the formula unit. The C_6-linkage in **4**–**7** is 1,6-hexanediyl. The *N*-substituents on the pyrrolidinium rings are methyl (**4**), ethyl (**5**), butyl (**6**) and allyl (**7**). Compound **4** crystallized as a mixture of two polymorphs (**4a** and **4b**) and both structures were determined crystallographically. The crystal systems in both **4a** and **4b** are triclinic with *P*-1 space groups. Both of these structures have two independent pentaborate anions and dications in which all atoms are crystallographically unique. Crystallographically, the cations in **5** and **7** are centrosymmetric and the two pentaborate anions are equivalent. In **6**, the two pentaborate anions are equivalent, the four $B(OH)_3$ molecules are crystallographically comprised of pairs of two independent molecules and all atoms in the cation are crystallographically unique. Drawings of the structures of **4a** and **4b** and **5**–**7** are given in Figures 5 and 6 respectively, together with details of their crystallographic atomic labels.

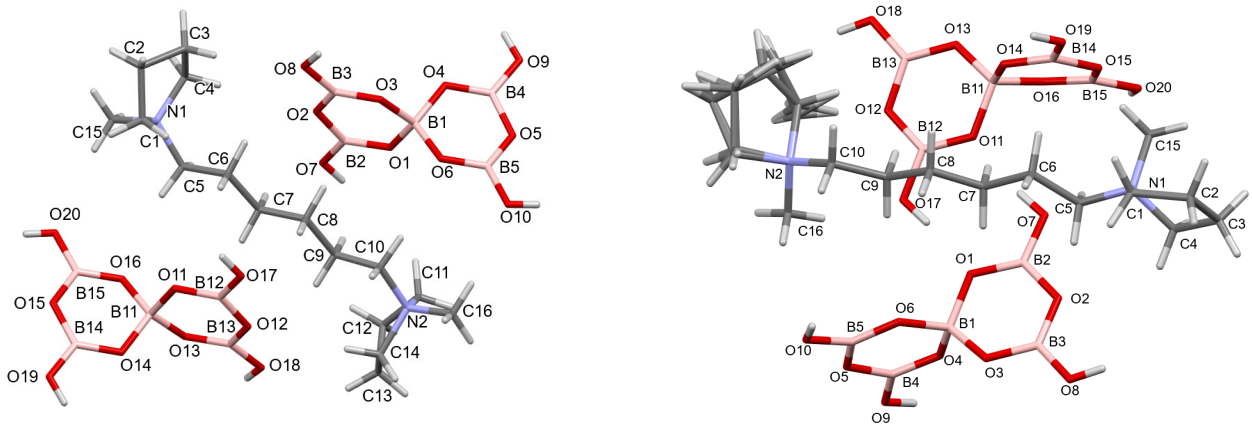

(**a**) (**b**)

Figure 5. Drawings of the structures of the two polymorphs of $[(C_4H_8N)(Me)(CH_2)_6(Me)(NC_4H_8][B_5O_6(OH)_4]_2$ showing selected atomic numbering (**a**) **4a**, and (**b**) **4b**. H atoms in the pentaborate anions have the same number as the heavy atom to which they are attached. The carbons of the pyrrolidinium ring containing N2 in **4b** are disordered. Full crystallographic atomic labelling is availablein the ESI.

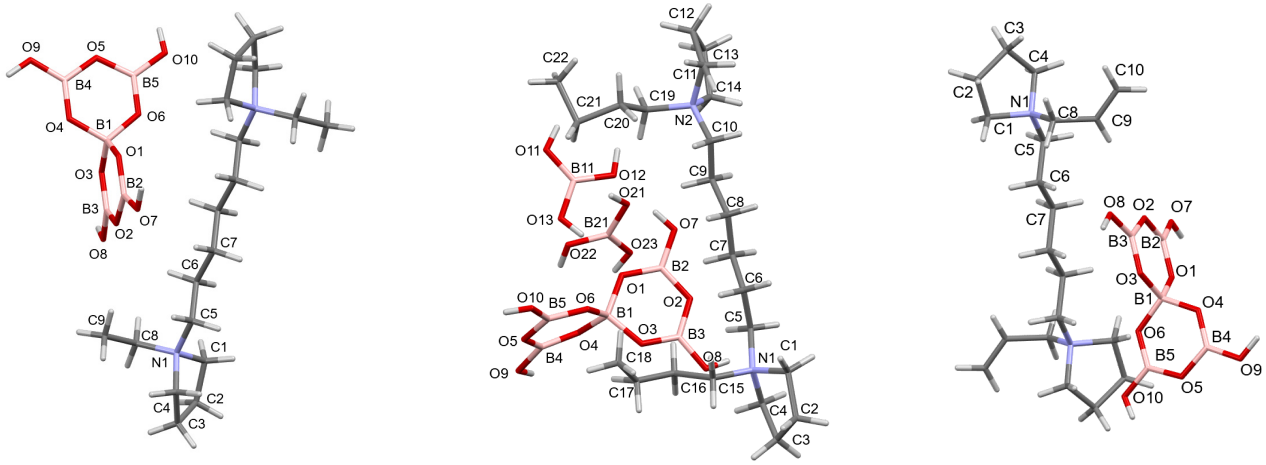

(**a**) (**b**) (**c**)

Figure 6. Drawings of the structures of (**a**) $[(C_4H_8N)(Et)(CH_2)_6(Et)(NC_4H_8][B_5O_6(OH)_4]_2$ (**5**), (**b**) $[(C_4H_8N)(Bu)(CH_2)_6(Bu)(NC_4H_8][B_5O_6(OH)_4]_2{\cdot}4B(OH)_3$ (**6**) and (**c**) $[(C_4H_8N)(allyl)(CH_2)_6(allyl)(NC_4H_8][B_5O_6(OH)_4]_2$ (**7**) showing selected crystallographic atomic numbering. H atoms labels are omitted for clarity and in the pentaborate anions have the same number as the heavy atom to which they are attached.

The bond distances and internuclear bond angles for the pyrrolidinium centres in the dications **4**–**7** are all similar to those reported for unlinked pyrrolidinium cations [23,29,30]. The 1,6-hexanediyl fragments linkages in **4**–**7** all adopt staggered 'zig-zag' conformations as was observed for **1** and **2**. The bond angles and bond distances within the pentaborate anions of **4**–**7** are within the ranges reported for other pentaborate salts and compounds containing boroxole rings with both 3- and 4-coordinate boron centres [15,17]. Thus, the OBO angles from 3-coordinate 'trigonal plane' boron centres [118.42(7)–123.01(7)° (**4a**); 115.63(11)–123.36(11)° (**4b**); 115.00(13)–124.72(13)° (**5**), 116.5(3)–122.0(3)° (**6**); 114.97(14)–124.44(14)° (**7**)] are larger than those involving the 4-coordinate 'tetrahedral' boron centres [107.70(7)–111.38(7)° (**4a**); 107.32(9)–112.00(9)° (**4b**); 107.96(10)–111.23(11)° (**5**), 107.6(3)–111.4(3)° (**6**); 108.41(10)–110.97(12)° (**7**)]. The distortion from idealized tetrahedral geometry can be quantified using τ_4 [55] and THC/100 [56] values. Calculated τ_4 values obtained for

4a, **4b**, **5**, **6**, and **7** were all 0.98. The calculated *THC*/100 values for these compounds ranged from 0.907 (**4a**, B11) to 0.937 (**7**). B-O distances involving 3-coordinate B centres [1.3541(11)–1.3907(12) Å (**4a**); 1.3504(16)–1.3903(15) Å (**4b**); 1.3375(19)–1.3986(19) Å (**5**), 1.348(5)–1.383(5) Å (**6**); 1.340(2)–1.3933(19) Å (**7**)] are shorter than those involving the 4-coordinate boron centres [1.4508(11)–1.4907(11) Å (**4a**); 1.4492(15)–1.4839(15) Å (**4b**); 1.4665(15)–1.4821(17) Å (**5**), 1.459(5)–1.471(5) Å (**6**); 1.4560(19)–1.4850(17) Å (**7**)]. The ranges of the boroxole ring BOB angles are 118.42(7)–123.01(7)° (**4a**), 119.06(10)–124.67(9)° (**4b**), 119.09(12)–124.00(11)° (**5**), 117.7(3)–123.3(3)° (**6**) and 118.90(12)–124.14(11)° (**7**), supporting possible sp^2 hybridization for these ring oxygen atoms [57]. Within the co-crystallized $B(OH)_3$ in **6** the B-O distances range from 1.356(6)–1.374(6) Å and the OBO angles range from 116.5(5)–124.4(5)°.

The cations in **4**–**7** are unable to form H-bonding interactions and the solid-state structures directing H-bond interactions in **4a**, **4b**, **5** and **7** are restricted to anion-anion interactions (see below). Compound **6** is co-crystallized with $4B(OH)_3$ and anion-$B(OH)_3$ H-bonding interactions are observed in this compound (see below).

The anionic lattices in polymorphs **4a** and **4b** are structurally very similar: in both structures the pentaborates are H-bond donors to $\alpha\alpha\alpha\beta$ sites of neighbouring pentaborate anions via 3 $R_2^2(8)$ interactions and chain interactions generating brick wall anionic lattices [15,29]. In both structures there are two independent pentaborate anions and both are $\alpha\alpha\alpha\beta$. In **4a** four of the $R_2^2(8)$ interactions are reciprocal whilst the other two link to two of the other independent pentaborate anions. There are two distinct C(8) chains in **4a** linking either pentaborates containing solely B1 centres or those containing solely B11 centres. In polymorph **4b** two of the six $R_2^2(8)$ interactions are reciprocal whilst the other four are linking the crystallographically independent pentaborate anions. The chain in **4b** links alternating independent pentaborate anions and is correctly described as a $C_2^2(16)$ rather than C(8). There is a noticeable difference in the cell volumes of the two polymorphs (1515.35(4) $Å^3$ and 1552.40(10) $Å^3$) with **4a** being the smaller. The cations also pack differently within the large channels of the two polymorphs; in **4a** they form overlapping diagonal strips across the channels (as seen in **3**) whereas in **4b** they sit as two chains parallel to each other and to the channels (as seen in **2**).

The crystal data (crystal system, space group, unit cell parameters) for **5** and **7** are very similar with unit cell volumes of 1740.10(3) $Å^3$ and 1791.50(13) $Å^3$, respectively; the cations in these salts only differ by the substituents on the pyrrolidinium rings (Et for **5** or allyl for **7**). As we have noted previously, anionic lattices are flexible and can easily adapt to small changes in cation size [23]. Therefore, and not unsurprisingly, the anionic giant lattices in **5** and **7** are structurally very similar and have identical pentaborate H-bonding arrangements with four $R_2^2(8)$ rings to $\alpha\alpha\alpha\gamma$ acceptor sites. This motif has been observed previously [15,29] and is also quite common. The α-$R_2^2(8)$ interactions that originate from the boroxole rings with γ-$R_2^2(8)$ interactions are reciprocal where $R_2^2(8)$ interactions from the other boroxole ring are not. Rectangular brick-like channels are observed when viewing down the *b* axis of **5** (and **7**) and the zig-zag cations sit diagonally within these channels (Figure 7).

The pentaborate salt **6** differs from **5** and **7** in that it is a co-crystal with four $B(OH)_3$ molecules per cation, i.e., $[(C_4H_8N)(Bu)(CH_2)_6(Bu)(NC_4H_8][B_5O_6(OH)_4]_2{\cdot}4B(OH)_3$ and the substituents on the pyrrolidine rings are n-butyl. The four $B(OH)_3$, represented by two independent $B(OH)_3$ molecules, are integrated into the pentaborate network with the result that there are now no inter-pentaborate $R_2^2(8)$ rings. Rather, each boroxole ring of the pentaborate anion has H-bonds to two $B(OH)_3$ molecules by $R_2^2(8)$ interactions (Figure 8). Due to the positions of their H-atoms the two $B(OH)_3$ molecules have C_s rather than C_{3h} symmetry. The $R_2^2(8)$ interactions originating from O7H7 and O9H9 to $B(OH)_3$ molecules containing B11 and B21, respectively, i.e., {-O7H7···O12B11O13H13···O1B2-} and {O9H9···O22B21O21H21···O4B4-}, are normal $R_2^2(8)$ interactions with one donor atom and one acceptor atom on each of the moieties. The H-atom positions in the $B(OH)_3$ molecules enables them to hydrogen bond in 'pincer' $R_2^2(8)$ motifs where the $R_2^2(8)$ donors are the $B(OH)_3$ and the acceptors are the boroxole rings {-O11H11···O3B3O8···H12O12B11-} and

{O23H23···O6B5O10···H22O22B21-}. Pincer $R_2^2(8)$ are well-known in polyborate/$B(OH)_3$ lattices [16,22,24,43–45]. The pentaborate pincer acceptor atoms, O8 and O10, are both part of hydroxyl groups and are involved in donor interactions as two C(8) chains involving only pentaborate atoms: {-O8′H8′···O9B4O4B1O3B3-}$_n$ and {O10′H10′···O7B2O1B1O6B5-}$_n$. The chains are linked via $B(OH)_3$ sites into $R_4^4(12)$ rings. This complex pentaborate/$B(OH)_3$ 3D lattice has rectangular channels that largely contain the cations (Figure 9). Overall, the structure is very similar to the diamondoid arrangement observed in $[N^nPr_4][B_5O_6(OH)_4]\cdot 2B(OH)_3$ and $[N^nBu_4][B_5O_6(OH)_4]\cdot 2B(OH)_3$ [43].

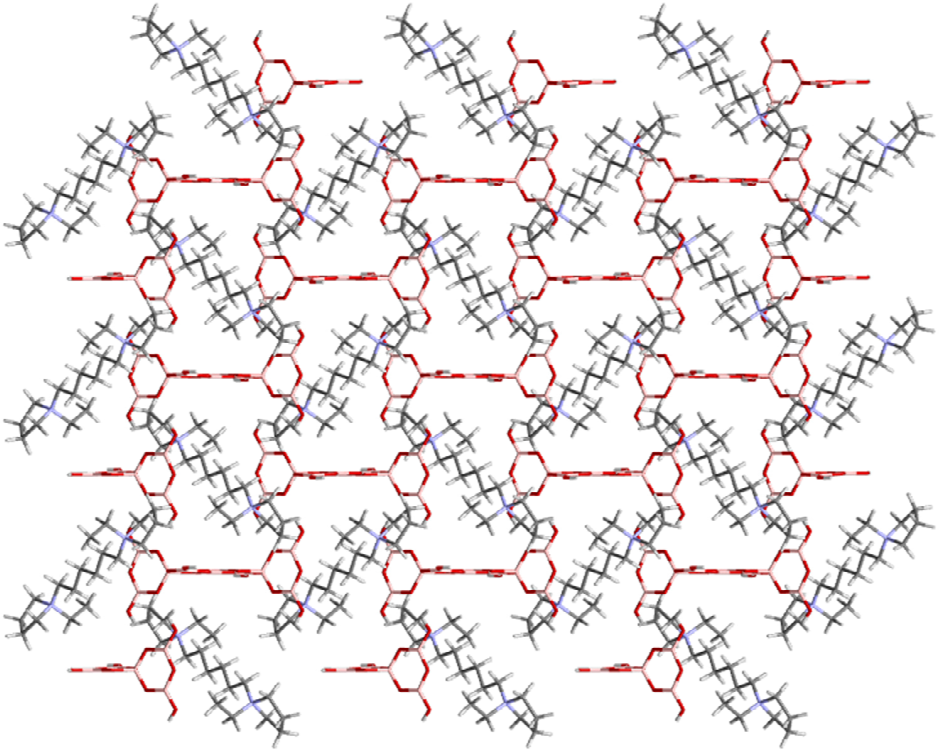

Figure 7. Diagram of the cation/anion lattice packing of $[(C_4H_8N)(Et)(CH_2)_6(Et)(NC_4H_8][B_5O_6(OH)_4]_2$ (**5**) when viewed down the *b*-axis. The cations sit slanting diagonally within the rectangular channels. The cation/anion lattice packing in $[(C_4H_8N)(allyl)(CH_2)_6(allyl)(NC_4H_8][B_5O_6(OH)_4]_2$ (**7**) is very similar.

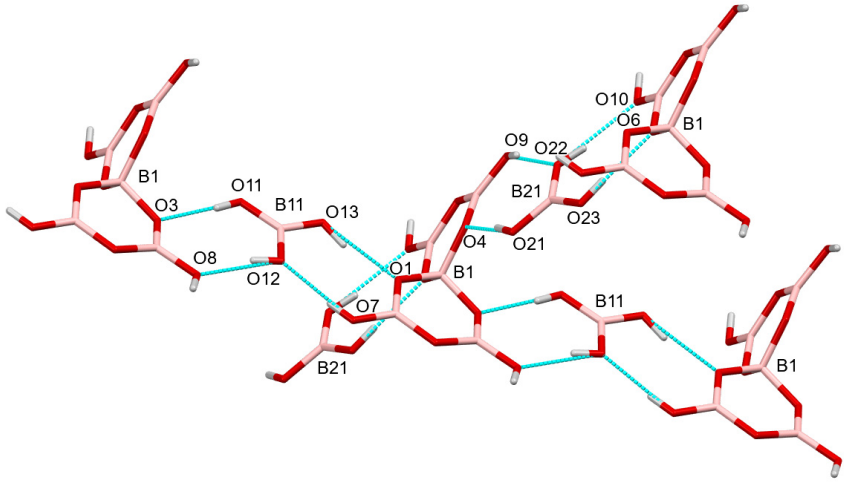

Figure 8. Diagram showing $B(OH)_3$ molecules in $[(C_4H_8N)(Bu)(CH_2)_6(Bu)(NC_4H_8][B_5O_6(OH)_4]_2\cdot 4B(OH)_3$ (**6**) connecting pentaborates in two planes parallel with the boroxole rings of the pentaborate anions.

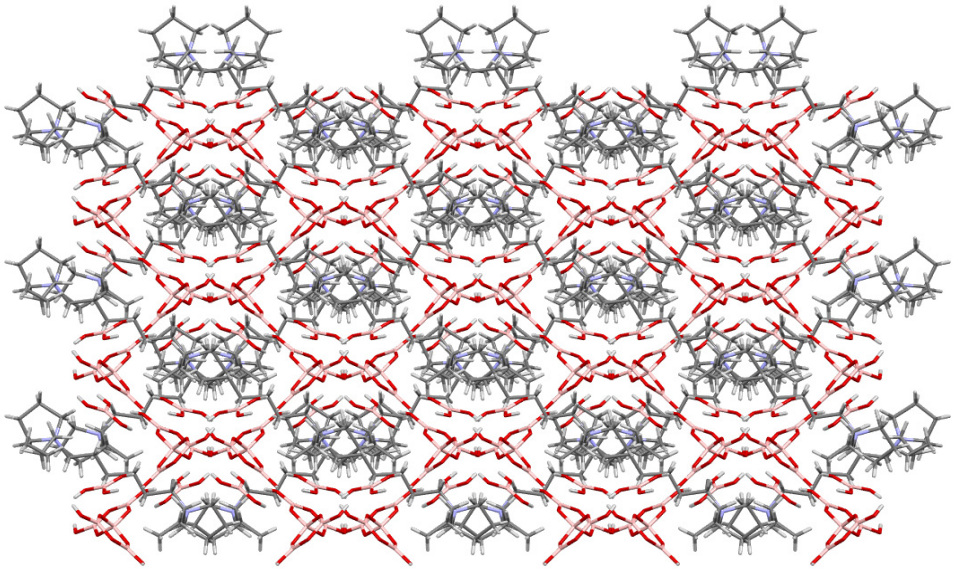

Figure 9. Packing diagram of $[(C_4H_8N)(Bu)(CH_2)_6(Bu)(NC_4H_8][B_5O_6(OH)_4]_2{\cdot}4B(OH)_3$ (**6**) viewed down the *c*-axis, showing the large rectangular channels occupied by the cations.

3. Experimental

3.1. General

All chemicals and reagents were purchased from Sigma Aldrich (Gillingham, UK), or Fisher Scientific (Loughborough, UK), and used as supplied without further purification. The halide salts, used as precursors to the pentaborate salts, were prepared by methods described in the literature [58–61]. NMR spectra were recorded at room temperature (298 K) on a Bruker Ultrashield^{TM} Plus 400 (Bruker, Coventry, UK), operating at 400 MHz for ^{1}H, 100 MHz for ^{13}C spectra using D_2O as an internal standard and at 128 MHz for ^{11}B, using $BF_3{\cdot}OEt_2$ as an external standard. NMR spectra were recorded using the Bruker TopSpin^{TM} 3.2 software package (Bruker, Coventry, UK). Infrared (FTIR) spectra were either obtained as KBr disks on a Perkin-Elmer 100 FTIR spectrometer (Perkin-Elmer, Seer Green, UK) over 400–4000cm^{-1}, or directly as powders using a Bruker Alpha Platinum ATR FTIR spectrometer (Bruker, Coventry, UK) over 375–4000cm^{-1}. Both devices ran 32 background and sample scans per experiment. Differential scanning calorimetry (DSC) and thermogravimetric analyses (TGA) were performed from room temperature to 800 °C in an air atmosphere on an SDT Q600 V4 Build 59 instrument (TA Instruments, New Castle, DE, USA) using Al_2O_3 crucibles with a ramp rate of 10 °C per minute. XRD crystallography was performed at the EPSRC national crystallographic centre at Southampton University. Drawing in the manuscripts have been generated using Mercury software (version 2022 2.0, CCDC, Cambridge, UK). Elemental analyses (C, H and N), were performed externally at OEA Laboratories Ltd. Callington, Cornwall, UK.

3.2. X-ray Crystallography

Crystallographic data are given in the experimental section and in the Supplementary Materials. Suitable crystals were selected and mounted on MITIGEN holders in perfluoroether oil and all crystals were kept at 100(2) K during data collection. Data collection [62] for all compounds, except **5**, were performed on a Rigaku FRE+ diffractometer equipped with either HF Varimax confocal mirrors (Chalgrove, UK), an AFC12 goniometer and a HG Saturn 724+ detector (**1**, **2**) or VHF Varimax confocal mirrors and an AFC12 goniometer and a HyPix 6000 detector (**3**, **4a, 4b, 6, 7**). Data collection for **5** was performed on a Rigaku 007HF diffractometer equipped with varimax confocal mirrors, an AFC11 goniometer and HyPix 6000 detector. Using Olex2 [63], the structures were solved with the ShelXT Structure solution programme [64] using the Intrinsic Phasing solution method. These models were refined using ShelXL using least squares minimisation [65].

3.3. Synthesis of Dication C_6-Linked Bispentaborate Salts

3.3.1. Preparation of 1,1′-(1,6-Hexanediyl)bis(3-methyl-1H-imidazol-3-ium)bispentaborate $[CH_3(C_3H_3N_2)(CH_2)_6(C_3H_3N_2)CH_3][B_5O_6(OH)_4]_2$ (**1**)

1,1′-(1,6-hexanediyl)bis(3-methyl-1H-imidazol-3-ium) diiodide (1.0 g, 2.0 mmol) was added to 16 g of DOWEX 550A ion exchange resin (OH^- form) and stirred for 18 h. The DOWEX was removed by vacuum filtration and the filtrate was added to 1.2 g (20 mmol) boric acid. The aqueous solution was stirred for 3 h and then evaporated under reduced pressure to yield a crude white solid (1.4 g, 2.0 mmol, 100%). An amount of 0.3 g of this solid was redissolved in 15 mL deionised water and recrystallized to yield a few white crystals (after 5 days) suitable for X-ray diffraction studies. $C_{14}H_{32}B_{10}N_4O_{20}$. Anal. Calc.: C = 24.6%, H = 4.7%, N = 8.2%. Found C = 24.9%, H = 4.7%, N = 8.1%. TGA: 250–400 °C, condensation of pentaborate units with loss of $4H_2O$ 11.6% (10.5% calc.); 400–800 °C, oxidation of organic cation to leave residual $5B_2O_3$ 45.7% (50.8% calc.). NMR/ppm: δ_H: 1.24 (4H, t, CH_2); 1.76, (4H, t, CH_2), 3.79 (6H, s, CH_3), 4.08 (4H, t, CH_2N), 4.70 (HOD), 7.36 (4H, d, CH); δ_B: 17.9 (77%), 13.2 (20%), 1.2 (3%); δ_C: 24.81 (CH_2), 28.99 (CH_2), 35.34 (CH_3), 49.29 (CH_2), 122.06 (CH), 123.45 (CH). FTIR (ATR, neat solid state, cm^{-1}): 3236 (br), 3125 (w), 3095 (w), 2942 (w), 2868 (w), 1575 (w), 1383 (m), 1298 (m), 1171 (m), 1072 (m), 1012 (m), 912 (vs), 834 (m), 772 (m), 721 (m), 651 (m), 624 (m), 473 (m). XRD crystallographic data: $C_{14}H_{32}B_{10}N_4O_{20}$, *M*r = 684.53, monoclinic, $P2_1/c$, a = 9.6754(2) Å, b = 16.7781(3) Å, c = 9.1677(2) Å, $\alpha = \gamma = 90°$, β = 92.680(2)°, V = 1486.61(5) $Å^3$, T = 100(2) K, Z = 2, Z' = 0.5 μ(MoKα) = 0.131 mm^{-1}, 20,877 reflections measured, 3403 unique (R_{int} = 0.0339) which were used in calculations. The final ωR_2 was 0.0851 (all data) and R_1 was 0.0335 (I > 2σ(I)).

3.3.2. Preparation of 1,1′-(1,6-Hexanediyl)bis(3-ethyl-1H-imidazol-3-ium)bispentaborate $[C_2H_5(C_3H_3N_2)(CH_2)_6(C_3H_3N_2)C_2H_5][B_5O_6(OH)_4]_2{\cdot}3H_2O$ (**2**)

1,1′-(1,6-hexanediyl)bis(3-ethyl-1H-imidazol-3-ium) dibromide (1.0 g 2.3 mmol) was added to 20 g of DOWEX 550A ion exchange resin (OH^- form) and stirred for 18 h. The DOWEX was removed by vacuum filtration and the filtrate was added to 1.4g (23 mmol) boric acid. The solution was stirred for 2 h, and then evaporated under reduced pressure to yield a crude powder (1.5 g, 2.0 mmol, 76%) which was subjected to FTIR and NMR studies. Recrystallization of 0.3 g of the crude product in water yielded a few white crystals (after 14 days) suitable for single crystal XRD studies. $C_{16}H_{42}B_{10}N_4O_{23}$. Anal. Calc.: C = 25.1%, H = 5.5%, N = 7.3%. Found C = 25.5%, H = 5.0%, N = 7.3%. NMR/ppm: δ_H: 1.24 (4H, m, CH_2), 1.41 (6H, t, CH_3), 1.78 (4H, m, CH_2), 4.12 (8H, dt, CH_2N), 4.70 (HOD), 7.39 (4H, m, CH); δ_B: 13.2 (7%), 17.2 (93%); δ_C: 14.36 (CH_3), 24.85 (CH_2), 28.99 (CH_2), 44.74 (CH_2), 49.32 (CH_2), 121.93 (CH), 122.13 (CH). FTIR (neat solid state, cm^{-1}): 3217 (br), 3092 (w), 2950 (w), 2870 (w), 1569 (w), 1397 (w), 1380 (m), 1300 (vs), 1169 (m), 1148 (w), 1076 (m), 1014 (s), 913 (vs), 817 (m), 802 (m), 741 (m), 722 (w), 705 (m), 642 (m), 475 (m), 460 (w). XRD crystallographic data: $C_{16}H_{42}B_{10}N_4O_{23}$, *M*r = 766.63, triclinic, *P*-1, a = 9.4616(4) Å, b = 9.4780(3) Å, c = 19.8856(8) Å, α = 86.483(3)°, β = 81.244(3)°, γ = 75.624(3)°, V = 1706.79(12) $Å^3$, T = 100(2) K, Z = 2, Z' = 1, μ(MoKα) = 0.129 mm^{-1}, 38,202 reflections measured, 7820 unique (R_{int} = 0.0424) which were used in calculations. The final ωR_2 was 0.1431 (all data) and R_1 was 0.0457 (I > 2σ(I)).

3.3.3. Preparation of 1,1′-[1,4-Phenylenebis(methylene)]bis(2-methyl-1H-imidazol-3-ium) bispentaborate $[CH_3(C_3H_3N_2)CH_2(C_6H_4)CH_2(C_3H_3N_2)CH_3][B_5O_6(OH)_4]_2$ (**3**)

1,1′-[1,4-Phenylenebis(methylene)]bis(2-methyl-1H-imidazol-3-ium) diiodide (1.0 g, 1.9 mmol) was added to DOWEX 550A monosphere $(OH)^-$ (15 g), and stirred for 18 h. The DOWEX was removed by vacuum filtration and the filtrate was added to boric acid (1.2 g, 19 mmol). The aqueous solution was stirred for 3 h and then evaporated under reduced pressure to yield a crude white solid (1.3 g, 1.8 mmol, 95%). An amount of 0.3 g of this solid was redissolved in 15 mL deionised water and recrystallized to yield a few white crystals (after 7 days) suitable for X-ray diffraction studies. $C_{16}H_{28}B_{10}N_4O_{20}$. Anal. Calc.: C = 27.3%, H = 4.0%, N = 7.9%. Found C = 27.5%, H = 4.0%, N = 7.9%. NMR: δ_H/ppm:

3.79 (6H, s, CH_3N), 4.70 (HOD), 5.32 (4H, s, CH_2N), 7.36 (8H, m, CH); δ_B: 1.2 (6.6%), 13.1 (29%), 18.1 (64%); δ_C: 35.68 (CH_3), 52.24 (CH_2), 122.22 (CH), 123.82 (CH), 129.21 (CH), 134.57 (C (quat). FTIR (KBr, cm^{-1}): 3439 (s), 3379 (s), 3142 (m), 3074 (m), 1647 (m), 1575 (m), 1435 (vs), 1360 (vs), 1252 (m), 1162 (m), 1103 (s), 1025 (s), 925 (vs), 782 (w), 698 (m). XRD crystallographic data: $C_{16}H_{28}B_{10}N_4O_{20}$, *M*r = 704.52, triclinic, *P*-1, a = 9.0501(2) Å, b = 9.1652(2) Å, c = 9.95476(2) Å, α = 104.254(2)°, β = 94.968(2)°, γ = 103.538(2)°, V = 737.43(3) $Å^3$, T = 100(2) K, Z = 1, Z' = 0.5, μ(MoKα) = 0.135 mm^{-1}, 44,644 reflections measured, 4490 unique (R_{int} = 0.0242) which were used in calculations. The final ωR_2 was 0.0890 (all data) and R_1 was 0.0312 (I > 2σ(I)).

3.3.4. Preparation of 1,1′-(1,6-Hexanediyl)bis(1-methylpyrrolidin-1-ium)bispentaborate $[CH_3(C_4H_8N)(CH_2)_6(C_4H_8N)CH_3][B_5O_6(OH)_4]_2$ (**4**)

1,1′-(1,6-hexanediyl)bis(1-methylpyrrolidin-1-ium) diiodide (1.0 g, 2.0 mmol) was added to DOWEX 550A monosphere $(OH)^-$ (17 g), and stirred for 24 h. The aqueous solution was collected and added to boric acid (1.2 g, 19 mmol). The solution was stirred for 2 h, and then the solution was evaporated under reduced pressure to yield a crude powder (1.3 g, 1.9 mmol, 95%). Recrystallisation of 0.3 g of the crude product from water yielded a few white crystals (after 7 days) suitable for XRD studies. These crystals were found to be two polymorphs. $C_{16}H_{42}B_{10}N_2O_{20}$. Anal. Calc.: C = 27.8%, H = 6.1%, N = 4.1%. Found C = 28.1%, H = 6.1%, N = 4.0%. NMR/ppm: δ_H: 1.35 (4H, m, CH_2); 1.74, (4H, t, CH_2), 2.12 (8H, s, CH_2), 2.95 (6H, s, CH_3N), 3.24 (4H, m, CH_2N), 3.42 (8H, m, CH_2N), 4.70 (HOD); δ_B: 1.1 (1%), 14.1 (13%), 17.3 (85%); δ_C: 21.20 (CH_2), 22.94 (CH_2), 25.26 (CH_2), 47.91 (CH_3), 63.95 (CH_2), 64.20 (CH_2). FTIR (KBr, cm^{-1}): 3233 (w,br), 1387 (m), 1297 (s), 1132 (m), 1009 (s), 908 (vs), 820 (m), 770 (s), 705 (s), 466 (m), 456 (m). XRD crystallographic data: (**4a**) $C_{16}H_{42}B_{10}N_2O_{20}$, M_r = 690.61, triclinic, *P*-1, a = 9.05340(10) Å, b = 11.9367(2) Å, c = 14.5824(2) Å, α = 94.1950(10)°, β = 104.1560(10)°, γ = 94.8550(10)°, V = 1515.35(4) $Å^3$, T = 100(2) K, Z = 2, Z' = 1, μ(MoK$_\alpha$) = 0.127 mm^{-1}, 69,149 reflections measured, 6954 unique (R_{int} = 0.0243) which were used in all calculations. The final wR_2 was 0.0906 (all data) and R_1 was 0.0314 (I > 2(I)). (**4b**) $C_{16}H_{42}B_{10}N_2O_{20}$, M_r = 690.61, triclinic, *P*-1 (No. 2), a = 9.6641(4) Å, b = 12.7484(4) Å, c = 13.0913(4) Å, α = 84.415(3)°, β = 84.541(3)°, γ = 75.872(3)°, V = 1552.40(10) $Å^3$, T = 100(2) K, Z = 2, Z' = 1, μ(MoK$_\alpha$) = 0.124 mm^{-1}, 35,495 reflections measured, 7118 unique (R_{int} = 0.0398) which were used in all calculations. The final wR_2 was 0.0929 (all data) and R_1 was 0.0358 (I > 2(I)).

3.3.5. Preparation of 1,1′-(1,6-Hexanediyl)bis(1-ethylpyrrolidin-1-ium)bispentaborate $[C_2H_5(C_4H_8N)(CH_2)_6(C_4H_8N)C_2H_5][B_5O_6(OH)_4]_2$ (**5**)

1,1′-(1,6-hexanediyl)bis(1-ethylpyrrolidin-1-ium) dibromide (0.9 g, 2.1 mmol) was added to DOWEX 550A monosphere $(OH)^-$ (18 g), and stirred for 18 h. The DOWEX was removed by vacuum filtration and the filtrate was added to boric acid (1.3 g, 21 mmol). The aqueous solution was stirred for 3 h and then evaporated under reduced pressure to yield a crude white solid (1.5 g, 2.1 mmol, 100%). An amount of 0.3 g of this solid was redissolved in 15 mL deionised water and recrystallized to yield a few white crystals (after 10 days) suitable for X-ray diffraction studies. $C_{18}H_{46}B_{10}N_2O_{20}$. Anal. Calc.: C = 30.1%, H = 6.5%, N = 3.9%. Found C = 28.1%, H = 6.2%, N = 3.6%. NMR/ppm: δ_H: 1.20 (6H, t, CH_3), 1.31 (4H, m, CH_2), 1.63 (4H, m, CH_2), 2.05 (8H, s, CH_2), 3.11 (4H, m, CH_2N), 3.24, (4H, q, CH_2N), 3.37 (8H, m, CH_2N); 4.70 (HOD); δ_B: 13.1 (9%), 17.4 (91%); δ_C: 7.91 (CH_3), 21.39 (CH_2), 22.38 (CH_2), 25.26 (CH_2), 54.76 (CH_2), 58.68 (CH_2), 62.24 (CH_2). FTIR (ATR, solid state, cm^{-1}): 3433 (br), 3363 (br), 1395 (s), 1297 (s), 1141 (w), 1104 (m), 1020 (m), 907 (s), 802 (w), 767 (s), 721 (m), 704 (vs), 457 (m). XRD crystallographic data: $C_{18}H_{46}B_{10}N_2O_{20}$, M_r = 718.67, monoclinic, $P2_1/c$, a = 10.06420(10) Å, b = 11.55510(10) Å, c = 15.7004(2) Å, β = 107.6290(10)°, $\alpha = \gamma$ = 90°, V = 1740.10(3) $Å^3$, T = 100(2) K, Z = 2, Z' = 0.5, μ(CuK$_\alpha$) = 0.976 mm^{-1}, 25,011 reflections measured, 3183 unique (R_{int} = 0.0306) which were used in all calculations. The final wR_2 was 0.1290 (all data) and R_1 was 0.0417 (I > 2(I)).

3.3.6. Preparation of 1,1′-(1,6-Hexanediyl)bis(1-butylpyrrolidin-1-ium) bispentaborate $[C_4H_9(C_4H_8N)(CH_2)_6(C_4H_8N)C_4H_9][B_5O_6(OH)_4]_2{\cdot}4B(OH)_3$ (**6**)

1,1′-(1,6-hexanediyl)bis(1-butylpyrrolidin-1-ium) diiodide (1.0 g, 1.7 mmol) was added to DOWEX 550A monosphere $(OH)^-$ (14 g), and stirred for 18 h. The DOWEX was removed by vacuum filtration and the filtrate was added to boric acid (1.0 g, 16.2 mmol). The aqueous solution was stirred for 3 h and then evaporated under reduced pressure to yield a crude white solid (1.7 g, 1.7 mmol, >100%). An amount of 0.3 g of this solid was redissolved in 15 mL deionised water and recrystallized to yield a few white crystals (after 7 days) suitable for X-ray diffraction studies. $C_{22}H_{66}B_{14}N_2O_{32}$. Anal. Calc.: C = 25.9%, H = 6.5%, N = 2.7%. Found C = 26.5%, H = 6.5%, N = 2.8%. NMR/ppm: δ_H: 0.83 (6H, t, CH_3); 1.27 (4H, m, CH_2), 1.58 (4H, s, CH_2), 2.05 (8H, s, CH_2), 3.11 (8H, t, CH_2N), 3.38 (8H, m, CH_2N), 4.70 (HOD); δ_B: 1.4 (<1%), 13.1 (14%), 18.0 (86%); δ_C: 12.74 (CH_3), 19.12 (CH_2), 21.40 (CH_2), 22.47 (CH_2), 24.53 (CH_2), 25.23 (CH_2), 59.36 (CH_2), 62.74 (CH_2). FTIR (ATR, solid state, cm^{-1}): 3316 (br), 1403 (m), 1306 (vs), 1225 (m), 1158 (m), 1128 (m), 1031 (m), 923 (s), 873 (m), 828 (s), 781 (m), 745 (w), 717 (w), 701 (m), 670 (m), 520 (w), 462 (m). XRD crystallographic data: $C_{22}H_{66}B_{14}N_2O_{32}$, M_r = 1022.10, monoclinic, *Cc*, a = 9.7545(3) Å, b = 15.4363(4) Å, c = 17.0325(5) Å, β = 101.851(3)°, $\alpha = \gamma$ = 90°, V = 2509.98(13) $Å^3$, T = 100(2) K, Z = 2, Z' = 0.5, $\mu(MoK_\alpha)$ = 0.117 mm^{-1}, 9481 reflections measured, 9481 unique (R_{int} = N/A) which were used in all calculations. The final wR_2 was 0.1483 (all data) and R_1 was 0.0532 (I > 2(I)).

3.3.7. Preparation of 1,1′-(1,6-Hexanediyl)bis(1-allylpyrrolidin-1-ium)bispentaborate $[C_3H_5(C_4H_8N)(CH_2)_6(C_4H_8N)C_3H_5][B_5O_6(OH)_4]_2$ (**7**)

1,1′-(1,6-hexanediyl)bis(1-allylpyrrolidin-1-ium) diiodide (1.0 g, 1.8 mmol) was added to DOWEX 550A monosphere $(OH)^-$ (16 g), and stirred for 18 h. The DOWEX was removed by vacuum filtration and the filtrate was added to boric acid (1.1 g, 18 mmol). The aqueous solution was stirred for 3 h and then evaporated under reduced pressure to yield a crude white solid (1.3 g, 1.8 mmol, 100%). An amount of 0.3 g of this solid was redissolved in 15 mL deionised water and recrystallized to yield a few white crystals (after 7 days) suitable for X-ray diffraction studies. $C_{20}H_{46}B_{10}N_2O_{20}$. Anal. Calc.: C = 32.3%, H = 6.2%, N = 3.8%. Found C = 29.7%, H = 5.9%, N = 3.3%. TGA: 110–800 °C simultaneous condensation of pentaborate units with loss of $4H_2O$ and oxidation of organic cation to leave residual $5B_2O_3$ 44.8% (46.9% calc.). NMR/ppm: δ_H: 1.32 (4H, m, CH_2); 1.71, (4H, t, CH_2), 2.10 (8H, s, CH_2), 3.17 (4H, s, CH_2N), 3.36 (4H, m, CH_2N), 3.47 (4H, m, CH_2N), 3.82 (4H, m, CH_2N), 4.70 (HOD), 5.61 (4H, m, CH_2 = C), 5.89 (2H, t, CH = C); δ_B: 1.2 (1%), 13.0 (20%), 17.3 (79%); δ_C: 21.39 (CH_2), 22.37 (CH_2), 25.20 (CH_2), 59.91 (CH_2), 61.41 (CH_2), 61.97 (CH_2), 125.07 (CH), 127.59 (CH_2). FTIR (KBr, cm^{-1}): 3406 (w), 3278 (m,br), 1392 (s), 1294 (s), 1137 (m), 1090 (m), 1056 (m), 1018 (s), 908 (vs), 769 (s), 706 (s), 472 (m), 459 (m). XRD crystallographic data: $C_{20}H_{46}B_{10}N_2O_{20}$, M_r = 742.69, monoclinic, $P2_1/c$, a = 10.0823(5) Å, b = 11.6950(4) Å, c = 15.7836(6) Å, β = 105.717(5)°, $\alpha = \gamma$ = 90°, V = 1791.50(13) $Å^3$, T = 100(2) K, Z = 2, Z' = 0.5, $\mu(MoK_\alpha)$ = 0.113 mm^{-1}, 22,100 reflections measured, 4090 unique (R_{int} = 0.0653) which were used in all calculations. The final wR_2 was 0.1324 (all data) and R_1 was 0.0449 (I > 2(I)).

4. Conclusions

A series of new C_6-linked *N*-substituted diimidazolium and dipyrrolidinium pentaborate salts have been synthesized by templated self-assembly reactions from $B(OH)_3$ in aqueous solution. TGA of **1** and **7** confirm that these compounds are thermally decomposed in air at 800 °C to B_2O_3. Their solid-state (XRD) structures show that the pentaborate anions are incorporated into giant H-bonded lattices, mainly through energetically favourable $R_2^2(8)$ interactions, with the associated cations largely innocent and situated within the channels. The solid-state structure of the co-crystal product **6**, $[C_4H_9(C_4H_8N)(CH_2)_6(C_4H_8N)C_4H_9][B_5O_6(OH)_4]_2{\cdot}4B(OH)_3$, is unusual in that there are no direct $R_2^2(8)$ anion-anion H-bonding interactions. However, within **6** there are sufficient

$B(OH)_3$ molecules to bridge all the pentaborate anions though a combination of standard $R_2^2(8)$ and pincer $R_2^2(8)$ H-bond interactions. The bridging $B(OH)_3$ molecules are also involved in $R_4^4(12)$ rings.

Supplementary Materials: The following supporting information can be downloaded at: https://www.mdpi.com/article/10.3390/inorganics12080220/s1. IR spectra (Figures S1–S7), NMR spectra (Figures S8–S25) and TGA plots (Figures S26 and S27) are available in the ESI. Crystallographic data for **1–3**, **4a**, **4b**, **5–7** are also available as ESI (Figures S28–S43 and Tables S1–S59). CCDC 2355367-23555374 respectively also contain the supplementary crystallographic data for this paper. These CCDC data can be obtained free of charge from CCDC, 12 Union Road, Cambridge, CB2 1EZ. Fax: +44 1223 336033; E-mail: deposit@ccdc.cam.ac.uk.

Author Contributions: Conceptualization, M.A.B., R.B. and T.A.R.; experimental methodology, T.A.R., A.R.A.-D. and P.N.H.; writing—original draft preparation, T.A.R. and M.A.B.; writing—review and editing, M.A.B. and P.N.H.; supervision, M.A.B.; funding acquisition, supervisor, S.J.C. All authors have read and agreed to the published version of the manuscript.

Funding: This research received no external funding.

Data Availability Statement: Crystallographic data available from CCDC, UK, see Supplementary Materials for details.

Acknowledgments: We thank the EPSRC for the NCS X-ray crystallography service (Southampton).

Conflicts of Interest: The authors declare no conflicts of interest.

References

1. Farmer, J.B. Metal borates. *Adv. Inorg. Chem. Radiochem.* **1982**, *25*, 187–237.
2. Heller, G. A survey of structural types of borates and polyborates. *Top. Curr. Chem.* **1986**, *131*, 39–98.
3. Topnikova, A.P.; Belokoneva, E.L. The structure and classification of complex borates. *Russ. Chem. Rev.* **2019**, *88*, 204–228. [CrossRef]
4. Christ, C.L.; Clark, J.R. A crystal-chemical classification of borate structures with emphasis on hydrated borates. *Phys. Chem. Miner.* **1977**, *2*, 59–87. [CrossRef]
5. Burns, P.C.; Grice, J.D.; Hawthorne, F.C. Borate minerals I. Polyhedral clusters and fundamental building blocks. *Can. Mineral.* **1995**, *33*, 1131–1151.
6. Burns, P.C. Borate clusters and fundamental building blocks containing four polyhedral: Why few clusters are utilized as fundamental building blocks of structures. *Can. Mineral.* **1995**, *33*, 1167–1176.
7. Grice, J.D.; Burns, P.C.; Hawthorne, F.C. Borate minerals II. A hierarchy of structures based upon the borate fundamental building block. *Can. Mineral.* **1999**, *37*, 731–762.
8. Touboul, M.; Penin, N.; Nowogrocki, G. Borates: A survey of main trends concerning crystal chemistry, polymorphism and dehydration process of alkaline and pseudo-alkaline borates. *Solid State Sci.* **2003**, *5*, 1327–1342. [CrossRef]
9. Belokoneva, E.L. Borate crystal chemistry in terms of extended OD theory: Topology and symmetry analysis. *Crystallogr. Rev.* **2005**, *11*, 151–198. [CrossRef]
10. Schubert, D.M.; Knobler, C.B. Recent studies in polyborate anions. *Phys. Chem. Glasses Eur. J. Glass Sci. Technol. B* **2009**, *50*, 71–78.
11. Schubert, D.M. Borates in industrial use. *Struct. Bond.* **2003**, *105*, 1–40.
12. Schubert, D.M. Boron oxide, boric acid, and borates. In *Kirk-Othmer Encyclopedia of Chemical Technology*, 5th ed.; J. Wiley Sons: New York, NY, USA, 2011; pp. 1–68.
13. Schubert, D.M. Hydrated zinc borates and their industrial uses. *Molecules* **2019**, *24*, 2419. [CrossRef]
14. Becker, P. Borate materials in nonlinear optics. *Adv. Mater.* **1998**, *10*, 979–992. [CrossRef]
15. Beckett, M.A. Recent Advances in crystalline hydrated borates with non-metal or transition-metal complex cations. *Coord. Chem. Rev.* **2016**, *323*, 2–14. [CrossRef]
16. Beckett, M.A.; Horton, P.N.; Hursthouse, M.B.; Timmis, J.L. Synthesis and thermal studies of two phosphonium tetrahydroxidohexa oxidooentaborate(1-) salts: Single-crystal XRD characterization of $[^iPrPPh_3][B_5O_6(OH)_4]\cdot 3.5H_2O$ and $[MePPh_3][B_5O_6(OH)_4]\cdot B(OH)_3\cdot 0.5H_2O$. *Molecules* **2023**, *28*, 6867. [CrossRef]
17. Xin, S.-S.; Zhou, M.-H.; Beckett, M.A.; Pan, C.-Y. Recent advances in crystalline oxidopolyborate complexes of d-block or p-block metals: Structural aspects, synthesis, and physical properties. *Molecules* **2021**, *26*, 3815. [CrossRef]
18. Desiraju, G.R. Supramolecular synthons in crystal engineering—A new organic synthesis. *Angew. Chem. Int. Ed. Engl.* **1995**, *34*, 2311–2327. [CrossRef]
19. Dunitz, J.D.; Gavezzotti, A. Supramolecular synthons: Validation and ranking of intermolecular interaction energies. *Cryst. Growth Des.* **2012**, *12*, 5873–5877. [CrossRef]

20. Sola, J.; Lafuente, M.; Atcher, J.; Alfonso, I. Constitutional self-selection from dynamic combinatorial libraries in aqueous solution through supramolecular interactions. *Chem. Commun.* **2014**, *50*, 4564–4566. [CrossRef]
21. Corbett, P.T.; Leclaire, J.; Vial, L.; West, K.R.; Wietor, J.-L.; Sanders, J.K.M.; Otto, S. Dynamic combinatorial chemistry. *Chem. Rev.* **2006**, *106*, 3652–3711. [CrossRef] [PubMed]
22. Beckett, M.A.; Coles, S.J.; Horton, P.N.; Jones, C.L. Polyborate anions partnered with large non-metal cations: Triborate(1-), pentaborate(1-) and heptaborate(2-) salts. *Eur. J. Inorg. Chem.* **2017**, *2017*, 4510–4518. [CrossRef]
23. Beckett, M.A.; Coles, S.J.; Davies, R.A.; Horton, P.N.; Jones, C.L. Pentaborate(1−) salts templated by substituted pyrrolidinium cations: Synthesis, structural characterization, and modelling of solid-state H-bond interactions by DFT calculations. *Dalton Trans.* **2015**, *44*, 7032–7040. [CrossRef] [PubMed]
24. Beckett, M.A.; Coles, S.J.; Horton, P.N.; Rixon, T.A. Structural (XRD) characterization and an analysis of H-bonding motifs in some tetrahydroxidohexaoxidopentaborate(1-) salts of N-substituted guandinium cations. *Molecules* **2023**, *28*, 3273. [CrossRef]
25. Beckett, M.A.; Brellocks, B.; Chizhevsky, I.T.; Damhus, T.; Hellwich, K.-H.; Kennedy, J.D.; Laitinen, R.; Powell, W.H.; Rabinovich, D.; Vinas, C.; et al. Nomenclature for boranes and related species (IUPAC Recommendations 2019). *Pure Appl. Chem.* **2020**, *92*, 355–381. [CrossRef]
26. Rixon, T.A. Stabilised Silicate and Borate Solutions for Foliar Agricultural Sprays. Ph.D. Thesis, Bangor University, Bangor, UK, 2019.
27. Beckett, M.A.; Coles, S.J.; Horton, P.N.; Rixon, T.A. Synthesis and XRD study of an C_2-linked bis(quaternary ammonium) pentaborate: $[Me_3NCH_2CH_2NMe_3][B_5O_6(OH)_4]_2$. *Phosphorus Sulfur Silicon Relat. Elem.* **2019**, *194*, 952–955. [CrossRef]
28. Beckett, M.A.; Meena, B.I.; Rixon, T.A.; Coles, S.J.; Horton, P.N. Pentaborate(1-) salts and a tetraborate(2-) salt derived from C_2- or C_3-linked bis(alkylammonium) dications: Synthesis, characterization and structural (XRD) studies. *Molecules* **2020**, *25*, 53. [CrossRef] [PubMed]
29. Beckett, M.A.; Horton, P.N.; Hursthouse, M.B.; Knox, D.A.; Timmis, J.L. Structural (XRD) and thermal (DSC, TGA) and BET analysis of materials derived from non-metal cation pentaborate salts. *Dalton Trans.* **2010**, *39*, 3944–3951. [CrossRef]
30. Jones, C.L.; Beckett, M.A.; Coles, S.J.; Davies, R.A.; Horton, P.N. Synthesis and characterization of templated pentaborate(1-) salts: X-ray structure of $[(2\text{-}HOCH_2CH_2)C_4H_7NMeH][B_5O_6(OH)_4]\cdot 0.3H_2O$. *Phosphorus Sulfur Silicon* **2016**, *191*, 628–630. [CrossRef]
31. Beckett, M.A.; Horton, P.N.; Hursthouse, M.B.; Timmis, J.L. Synthesis and X-ray structural studies of pentaborate(1-) salts containing substituted imidazolium cations. *Polyhedron* **2014**, *77*, 96–102. [CrossRef]
32. Han, W.-H.; Dang, L.-L.; Zhang, W.-J. Crystal structure of imidazolium tetrahydroxohexaoxopentaborate, $[C_3H_5N_2][B_5O_6(OH)_4]$. *Z. Kristallogr. NCS* **2007**, *222*, 403–404. [CrossRef]
33. Yang, H.-X.; Zhang, W.-J.; Liu, X.-L.; Liu, Z.-K. 2-Methimidazolium tetrahydroxohexaoxopentaborate. *Acta Cryst.* **2006**, *E62*, o4877–o4879.
34. Parker, T.G.; Pubbi, D.; Beehler, A.; Albrecht-Schmitt, T.E. 1-Ethyl-3-methyl-1H-imidazol-3-ium spiropentaborate. *Acta Cryst.* **2014**, *E70*, o171–o172. [CrossRef] [PubMed]
35. Visi, M.Z.; Knobler, C.B.; Owen, J.J.; Khan, M.I.; Schubert, D.M. Structures of self-assembled nonmetal borates derived from α,ω-diaminoalkanes. *Cryst. Growth Des.* **2006**, *6*, 538–545. [CrossRef]
36. Schubert, D.M.; Visi, M.Z.; Knobler, C.B. Guanidinium and imidazolium borates containing the first examples of an isolated nonaborate oxoanion: $[B_9O_{12}(OH)_6]^{(3-)}$. *Inorg. Chem.* **2000**, *39*, 2250–2251. [CrossRef]
37. Schubert, D.M.; Smith, R.A.; Visi, M.Z. Studies of crystalline non-metal borates. *Glass Technol.* **2003**, *44*, 63–70.
38. Etter, M.C. Encoding and decoding hydrogen-bond patterns of organic chemistry. *Acc. Chem. Res.* **1990**, *23*, 120–126. [CrossRef]
39. Salentine, G. High-field ^{11}B NMR of alkali borates. Aqueous polyborate equilibria. *Inorg. Chem.* **1983**, *22*, 3920–3924. [CrossRef]
40. Anderson, J.L.; Eyring, E.M.; Whittaker, M.P. Temperature jump rate studies of polyborate formation in aqueous boric acid. *J. Phys. Chem.* **1964**, *68*, 1128–1132. [CrossRef]
41. Liu, H.; Liu, Q.; Lan, Y.; Wang, D.; Zhang, L.; Tang, X.; Yang, S.; Luo, Z.; Tian, G. Speciation of borate in aqueous solution studied experimentally by potentiometry and Raman spectroscopy and computationally by DFT calculations. *New J. Chem.* **2023**, *47*, 8499–8506. [CrossRef]
42. Durka, K.; Jarzembska, K.N.; Kaminski, R.; Lulinski, S.; Serwatowski, J.; Wozniak, K. Structure and energetic landscapes of fluorinated 1,4-phenylboronic acids. *Cryst. Growth Des.* **2012**, *12*, 3720–3734. [CrossRef]
43. Freyhardt, C.C.; Wiebcke, M.; Felsche, J.; Englehardt, G. $N(n\text{Pr})_4[B_5O_6(OH)_4][B(OH)_3]_2$ and $N(n\text{Bu})_4[B_5O_6(OH)_4][B(OH)_3]_2$: Clathrates with a diamondoid arrangement of hydrogen bonded pentaborate anions. *J. Incl. Phenom. Mol. Recogn. Chem.* **1994**, *18*, 161–175. [CrossRef]
44. Beckett, M.A.; Horton, P.N.; Hursthouse, M.B.; Timmis, J.L.; Varma, K.S. Templated heptaborate and pentaborate salts of cyclo-alkylammonium cations: Structural and thermal properties. *Dalton Trans.* **2012**, *41*, 4396–4403. [CrossRef]
45. Beckett, M.A.; Horton, P.N.; Coles, S.J.; Kose, D.A.; Kreuziger, A.-M. Structural and thermal studies of non-metal cation pentaborate salts with cations derived from 1,5-diazobicyclo[4.3.0]non-5-ene, 1,8-diazobicyclo[5.4.0]undec-7-ene and 1,8-bis(dimethylamino)naphthalene. *Polyhedron* **2012**, *38*, 157–161. [CrossRef]
46. Yang, Y.; Fu, D.; Li, G.; Zhang, Y. Synthesis, crystal structure, and variable-temperature-luminescent property of the organically templated pentaborate $[C_{10}N_2H_9][B_5O_6(OH)_4].H_3BO_3\cdot H_2O$. *Z. Anorg. Allg. Chem.* **2013**, *639*, 722–727. [CrossRef]
47. Rajkumar, T.; Ranga Rao, G. Synthesis and characterization of hybrid molecular material prepared by ionic liquid and silicotungstic acid. *Mater. Chem. Phys.* **2008**, *112*, 853–857. [CrossRef]

48. Li, J.; Xia, S.; Gao, S. FT-IR and Raman spectroscopic study of hydrated borates. *Spectrochim. Acta* **1995**, *51A*, 519–532.
49. Babushkina, O.B. Phase Behaviour and FTIR Spectra of Ionic Liquids: The Mixtures of 1-Butyl-1-methylpyrrolidinium Chloride and $TaCl_5$. *Z. Naturforsch.* **2008**, *63A*, 66–72. [CrossRef]
50. Wang, G.-M.; Sun, Y.-Q.; Yang, G.-Y. Syntheses and crystal structures of two new organically templated borates. *J. Solid. State Chem.* **2004**, *177*, 4648–4654. [CrossRef]
51. Pan, C.-Y.; Zhong, L.-J.; Lu, J.; Li, D.-G.; Zhoa, F.-H.; Yang, H.-M. Synthesis, structure, and luminescent property of the templated borate $[C_9H_{14}N]\cdot[B_5O_6(OH)_4]$. *Z. Anorg. Allg. Chem.* **2014**, *640*, 352–356. [CrossRef]
52. Yang, S.; Li, G.; Tian, S.; Liao, F.; Lin, J. Synthesis and structure of $[C_2H_{10}N_2][B_5O_8(OH)]$: A nonmetal pentaborate with nonlinear optical properties. *Cryst. Growth Des.* **2007**, *7*, 1246–1250. [CrossRef]
53. Liu, H.-X.; Liang, Y.-X.; Jiang, X. Synthesis, crystal structure and NLO property of a nonmetal pentaborate $[C_6H_{13}N_2][B_5O_6(OH)_4]$. *J. Solid State Chem.* **2008**, *181*, 3243–3247. [CrossRef]
54. Luo, W.; Wang, Y.; Wen, T.; Zhang, H.; Lin, X.; Wang, Y.; Liao, F.; Lin, J. Synthesis, crystal structure and visible light emission of a new inorganic-organic hybrid pentaborate, $[C_6H_{12}N][B_5O_6(OH)_4]$. *J. Mol. Struct.* **2013**, *1048*, 1–5. [CrossRef]
55. Yang, L.; Powell, D.R.; Houser, R.P. Structural variation in copper(I) complexes with pyridylmethylamide ligands: Structural analysis with a new four-coordinate geometry index, τ_4. *Dalton Trans.* **2007**, *9*, 955–964. [CrossRef]
56. Hopfl, H. The tetrahedral character of the boron atom newly defined—A useful tool to evaluate the N→B bond. *J. Organomet. Chem.* **1999**, *581*, 129–149. [CrossRef]
57. Beckett, M.A.; Brassington, D.S.; Owen, P.; Hursthouse, M.B.; Light, M.E.; Malik, K.M.A.; Varma, K.S. p-Bonding in B-O ring species: Lewis acidity of $Me_3B_3O_3$, synthesis of amine $Me_3B_3O_3$ adducts, and the crystal and molecular structure of $Me_3B_3O_3\cdot NH_2{}^{i}Bu\cdot MeB(OH)_2$. *J. Organonmet. Chem.* **1999**, *585*, 7–11. [CrossRef]
58. Vlahakis, J.Z.; Mitu, S.; Roman, G.; Rodriguez, E.P.; Crandall, I.C.; Szarek, W.A. The anti-malarial activity of imidazolium salts. *Biorgan. Med. Chem.* **2011**, *19*, 6525–6542. [CrossRef] [PubMed]
59. Libman, D.D.; Pain, D.L.; Slac, R. Some bisquaternary salts. *J. Chem. Soc.* **1952**, 2305–2307. [CrossRef]
60. Cabildo, P.; Sanz, D.; Claramunt, R.M.; Bourne, S.A.; Alkorta, I.; Elguero, J. Synthesis and Structural Studies of Some [14]Paracyclo-bis-(1,2)pyrazolium- and (1,3)imidazolium-phanes. *Tetrahedron* **1999**, *55*, 2327–2340. [CrossRef]
61. Kobialka, S.; Müller-Tautges, C.; Schmidt, M.T.S.; Schnakenburg, G.; Hollóczki, O.; Kirchner, B.; Engeser, M. Stretch out or fold-back? Conformations of Dinuclear Gold(I) *N*-Heterocyclic Carbene Macrocycles. *Inorg. Chem.* **2015**, *54*, 6100–6111. [CrossRef]
62. Rigaku. *CrysAlisPro Software System*; Rigaku Oxford Diffraction; Rigaku Corporation: Cedar Park, TX, USA, 2019.
63. Dolomanov, O.V.; Bourhis, L.J.; Gildea, R.J.; Howard, J.A.K.; Puschmann, H. *Olex2*: A complete structure solution, refinement and analysis program. *J. Appl. Cryst.* **2009**, *42*, 339–341. [CrossRef]
64. Sheldrick, G.M. *ShelXT*-intergrated space-group and crystal structure determination. *Acta Cryst.* **2015**, *A71*, 3–8. [CrossRef]
65. Sheldrick, G.M. Crystal structure refinement with ShelXL. *Acta Cryst.* **2015**, *C71*, 3–8.